

On-Chip CNN Accelerator for Image Super-Resolution

Jung-Woo Chang and Suk-Ju Kang

Dept. of Electronic Engineering, Sogang University, Seoul, South Korea
{zwzang91, sjkang}@sogang.ac.kr

ABSTRACT

To implement convolutional neural networks (CNN) in hardware, the state-of-the-art CNN accelerators pipeline computation and data transfer stages using an off-chip memory and simultaneously execute them on the same timeline. However, since a large amount of feature maps generated during the operation should be transmitted to the off-chip memory, the pipeline stage length is determined by the off-chip data transfer stage. Fusion architectures that can fuse multiple layers have been proposed to solve this problem, but applications such as super-resolution (SR) require a large amount of an on-chip memory because of the high resolution of the feature maps. In this paper, we propose a novel on-chip CNN accelerator for SR to optimize the CNN dataflow in the on-chip memory. First, the convolution loop optimization technique is proposed to prevent using a frame buffer. Second, we develop a combined convolutional layer processor to reduce the buffer size used to store the feature maps. Third, we explore how to perform low-cost multiply-and-accumulate operations in the deconvolutional layer used in SR. Finally, we propose a two-stage quantization algorithm to select the optimized hardware size for the limited number of DSPs to implement the on-chip CNN accelerator. We evaluate our proposed accelerator with FSRCNN, which is most popular as the CNN-based SR algorithm. Experimental results show that the proposed accelerator requires 9.21ms to achieve an output image with the 2560×1440 pixel resolution, which is 36 times faster than the conventional method. In addition, we reduce the on-chip memory usage and DSP usage by 4 times and 1.44 times, respectively, compared to the conventional methods.

1 INTRODUCTION

Image super-resolution (SR) and computer vision [1, 2], such as object detection and recognition, have attracted much attention due to the emergence of convolutional neural networks (CNN). As a result, CNN accelerators have been studied extensively to apply various CNN algorithms to the real-time embedded systems. Especially, in hardware implementation, FPGA-based CNN accelerators are more energy efficient than those based on GPUs and can perform massive parallel processing than those based on CPUs [3, 4, 5, 6, 7].

CNN algorithms are difficult to store all necessary data with an on-chip memory except binary feature maps [7] because of the 3-D feature maps generated at each time the convolutional layer is processed. Therefore, most FPGA-based CNN accelerators use an off-chip memory and perform off-chip data transfer and computation simultaneously through ping-pong operations [3, 5, 6, 8]. As a result, a multiply-accumulate operation (MAC) is performed continuously through a convolutional layer processor

(CLP) with loop optimization techniques [3, 4, 5, 6, 8, 9]. Even if ping-pong operations are applied through double buffers, CLP cannot perform the next operation until a large amount of output feature maps are stored in the off-chip memory. In this case, the performance of the accelerators is degraded [6, 8]. Previous studies propose CNN fusion architectures to reduce large amounts of off-chip data transfer [6, 8]. Fusion architectures are designed as multi-CLPs for processing multiple convolutional layers within the CNN [6, 8]. Therefore, the data generated after CLP is executed is transferred to the next layer processor using the on-chip memory. In addition, the off-chip data transfer occurs only in the first layer and the last layer of the fused layers. However, in real-time applications for the image processing such as SR converting the low resolution (LR) images into high resolution (HR) images, the input and output buffers are difficult to be designed using line buffers because feature maps require a large amount of on-chip memory. On the other hand, a method for transforming deconvolutional layer into convolutional layer (TDC) is proposed to effectively parallelize deconvolutional neural networks (DCNN) that generate HR images from LR images [9]. In this method, several pixels in the output feature maps are generated in parallel by a convolution kernel which is smaller than a deconvolution kernel size. However, zero weights of converted convolution kernel are not considered, thereby performing unnecessary MAC operations.

In this paper, we propose a novel on-chip memory based CNN accelerator for the efficient data transfer. The main contributions of this paper are as follows.

- We propose a novel convolution loop optimization technique to implement the CNN accelerator with the on-chip memory.
- We develop the combined CLP architecture that combines consecutive CLPs to solve the problem of storing large amounts of feature maps in the limited buffer size.
- We explore how to design the CLP designed with the TDC method in the deconvolutional layer into the limited hardware resources of FPGA.
- We propose a two-stage quantization algorithm to reduce the size of the CNN in order to implement the designed on-chip CNN accelerator through the target FPGA.

2 BACKGROUND

2.1 CNN-based SR Algorithms

CNN-based SR algorithms are typically performed in two cases. In the first case for methods including SRCNN [2] and SRCNN-Ex [11], an input image is processed by the bicubic interpolation [10]

```

computation ( ):
for (i = 0; i < Kl; i++)
  for (j = 0; j < Kl; j++)
    for (tyy = y; tyy < min(y+Ty, Hl); tyy++)
      for (txx = x; txx < min(x+Tx, Wl); txx++)
        for (tmm = m; tmm < min(m+Tm, Ml); tmm++) #UNROLL
          for (tnn = n; tnn < min(n+Tn, Nl); tnn++) #UNROLL
            output_fml[tmm][tyy][txx] +=
              weightsl[tmm][tnn][i][j] ×
              input_fml[tnn][Sl × tyy + i][Sl × txx + j]

main ( ):
for (l = 0; l < L; l++)
  for (y = 0; y < Hl; y += Ty)
    for (x = 0; x < Wl; x += Tx)
      for (m = 0; m < Ml; m += Tm)
        for (n = 0; n < Nl; n += Tn) #DATAFLOW
          read_weights ( // load weightsl[Tm][Tn][Kl][Kl]
          read_bias ( // load biasl[Tm]
          read_input ( // load input_fml[Tn][Ty][Tx]
          computation (
          save_output ( // store output_fml[Tm][Ty][Tx]

```

Figure 1: Pseudo code of the accelerator with the conventional loop optimization techniques

to generate the HR image, and then CNN algorithms are performed. However, since the total execution cycles of the CNN accelerators are proportional to the resolution of the input image, the performance of the CNN accelerator is degraded by a scale factor. In the second case for the methods including FSRCNN and FSRCNN-s [12], the HR image is directly generated from the LR image using a deconvolutional layer. However, the deconvolutional layer is slower than the convolutional layer because it has more loop iterations than the convolutional layer [9]. But, it can be converted to the convolutional layer through the TDC method to improve the performance.

Generally, CNN-based algorithms require a large amount of the model size. The largest model size of the CNN algorithms mentioned above is 230 KB, and the model size of the CNN-based SR algorithms is small enough to be stored in the on-chip memory. Therefore, it is not necessary to use a model compression [13].

2.2 Conventional CNN Accelerators

Most CNN accelerators use loop optimization techniques to accelerate convolutional layers consisting of many stages of convolution loops [3, 4, 5, 6, 8, 9]. The pseudo code in Figure 1 shows an example of applying the loop optimization techniques. In *computation()*, the convolution loops are executed in parallel with the size of tile parameters through the *UNROLL* directive. The intermediate data generated by the processor are too large to be stored in the on-chip memory until the layer is completely processed. Therefore, conventional CNN accelerators solve the memory shortage problem through the off-chip memory [3, 4, 5, 6, 8, 9]. In *main()*, computation and off-chip data transfer stages are performed simultaneously on the same timeline through the *DATAFLOW* directive. However, since the pipeline stage length is limited by the off-chip data transfer, the use of the off-chip memory is a major bottleneck in the performance of the accelerators.

Fusion architectures are proposed to reduce the off-chip data transfer [6, 8]. Alwani et al. [6] propose a method of storing the last feature maps into the off-chip memory after performing computation in fused convolutional layers. Specifically, the resolution of feature maps is decreased when passing through the convolutional layer, and the final feature maps are stored in the off-

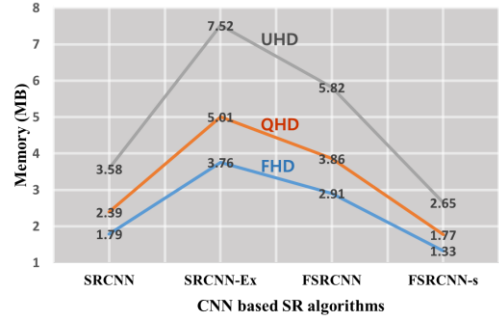


Figure 2: Required size of the line buffers for each CNN-based SR algorithms

chip memory. However, since the on-chip data transfer between fused layers is managed by the tile-based buffer approach, there is a burden that exception handling must be accompanied for various boundary conditions. To solve this problem, Xiao et al. [8] propose a method of managing feature maps as line buffers. Even if there are boundaries that require exception handling, data can be easily reused by using several line buffers. However, as the CNN-based SR algorithm has the high resolution of feature maps, the line buffers are difficult to be exploited due to the burden on the on-chip memory.

Unlike the convolutional layer, the deconvolutional layer has the process of accumulating kernel-sized output blocks in the previously obtained output feature maps. To implement this in hardware, it is necessary to carry out a complicated process of loading the output block stored in the memory into the buffer, adding it, and storing it again in the memory. The TDC method solves this problem by generating an output block with a fixed size that does not overlap with other output blocks. In addition, there is an advantage that all the pixels in the output block can be processed in parallel by the convolution. However, when converting from the deconvolutional layer to the convolutional layer, the newly created convolution kernel contains a large amount of weights with zero coefficients. Thus, we need to remove the operations for zero coefficients to enhance the FPGA resource utilization.

3 Proposed ARCHITECTURE DESIGN

3.1 Dataflow Optimization

In our system, the pixel data is sent to the FPGA through the display driver in the horizontal direction of the frame. When all the pixels in the frame have been transferred, the data for the next frame is sent to the FPGA. If all the convolutional layers are executed by the single CLP, the pixel data coming into the FPGA must be stored in the on-chip memory until the last layer is completely processed. Consequently, several frame buffers may be required depending on the execution time of the CLP. In order to solve this problem, we process input data coming into the FPGA by designing all the convolutional layers to run concurrently through the multiple CLPs such as the fusion architectures. In this case, the design of the multi-CLPs that can handle efficient on-chip dataflow is required. Thus,

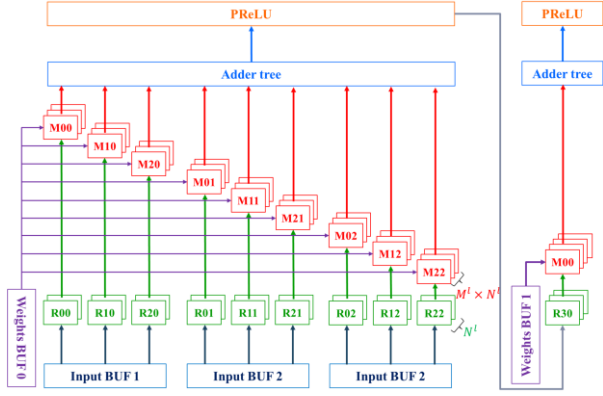


Figure 3: Proposed combined CLP architecture fused with the forward layer and the shrinking layer

we must determine the loop tiling parameters of each CLPs. To find the loop tiling parameters, we compare the computation speed of each CLP with the speed of the pixel data coming into the CLP.

The computation to transmission (CT) ratio is defined as the ratio of the cycles required to perform the l^{th} CLP to the cycles required to transmit the pixel data from the display driver or input buffers into the l^{th} CLP. When the tile size combination of the l^{th} CLP is given as T_y^l , T_x^l , T_m^l , T_n^l , and T_k^l , which denote the tile size of row, column, output feature maps, input feature maps, and kernel, the l^{th} CT, which is CT^l , is calculated by Equation (1). In this case, we do not consider T_y^l and T_x^l when calculating the CT^l because the input of each CLP is sequentially transmitted in pixel data instead of tile-sized pixel block.

$$CT^l \text{ ratio} = \frac{\text{total number of execution cycles}}{\text{total number of transmission cycles}} = \frac{H^l \times W^l \times \left\lceil \frac{M^l}{T_m^l} \right\rceil \times \left\lceil \frac{N^l}{T_n^l} \right\rceil \times \left\lceil \frac{K}{T_k^l} \right\rceil \times \left\lceil \frac{K^l}{T_k^l} \right\rceil}{H^l \times W^l \times \left\lceil \frac{N^l}{T_n^l} \right\rceil} \quad (1)$$

$$= \left\lceil \frac{M^l}{T_m^l} \right\rceil \times \left\lceil \frac{K^l}{T_k^l} \right\rceil \times \left\lceil \frac{K^l}{T_k^l} \right\rceil$$

where H^l and W^l are the height and width of feature maps, respectively, N^l and M^l are the size of the input and output feature maps, respectively, and K^l is the width of the kernel size in the l^{th} convolutional layer.

If the CT^l is greater than 1, the transmission speed of the pixel data is faster than that of the CLP, and hence, the data transferred during the computation must be stored in the frame buffer. For example, if an output image with the 1920×1080 (FHD) pixel resolution is generated using a SR algorithm with the scale factor of 2, a 4.15MB buffer memory is required to store an input image with the 960×540 pixel resolution in 32-bit floating point data type. In addition, considering the size of input feature maps, it can exceed the allowable on-chip memory of a typical FPGA. Therefore, we set the CTR of all layers to 1 not to use the frame buffer. Thus, T_m^l and T_k^l become M^l and K^l , respectively. Furthermore, the tiling factors of the input feature maps of the next

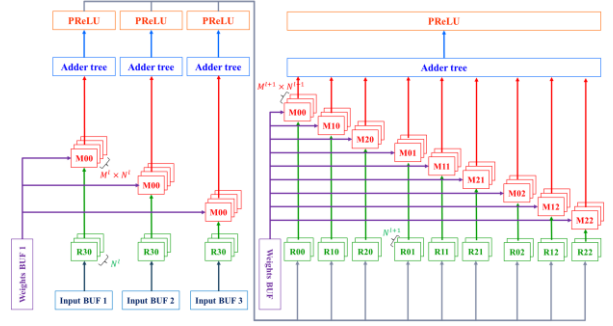


Figure 4: Proposed combined CLP architecture fused with the expanding layer and the backward layer

layer, T_n^{l+1} and T_m^l should be same for feature maps to be transmitted without buffering to the next layer. Since N^{l+1} is equal to M^l , T_n^l also becomes equal to N^l . As a result, all CLPs can fully process the three convolution loops in parallel.

3.2 Combined CLP Design

A memory management technique is needed to efficiently store feature maps generated by multi-CLPs. Since the pixel data from the display driver is transmitted line by line, we use the line buffer that can reuse the data without being restricted by boundary conditions [8]. The line buffer is designed as a block RAM (BRAM) that is a simple dual-port mode [14] in which one read and one write are allowed concurrently in order to fulfill both input and output buffers of each CLPs. In addition, the capacity needed to implement the line buffer should be same as the size of the 3-D data generated from the CLP. The number of line buffers must be equal to the kernel size for the convolution. Therefore, the size of the input and output buffers for the l^{th} CLP, which are M_{in}^l and M_{out}^l respectively, can be calculated by Equation (2).

$$M_{in}^l = K^l \times W^l \times N^l \times \text{pixel_datawidth} \quad (2)$$

$$M_{out}^l = K^{l+1} \times W^{l+1} \times N^{l+1} \times \text{pixel_datawidth}$$

Figure 2 shows the size of the line buffers required to generate output images with the output resolutions of FHD, 2560×1440 (QHD), and 3840×2560 (UHD) when using CNN-based SR algorithms [2, 10, 11]. FSR CNN-s, which requires the smallest amount of memory, should use 2.65MB memory to generate UHD image. These buffers are constructed with 588 numbers of 36K-BRAMs. Since it is larger than the number of the BRAMs available in general FPGAs, the required line buffers should be reduced.

We can solve the memory shortage problem through the shrinking and expanding layers, which are both 1×1 convolutional layers. The shrinking layer compresses the largest input feature maps to a reduced size. Conversely, the expanding layer restores the reduced size of the input feature maps back to the original size. Figure 3 shows the combined CLP with the fusion of the forward layer processor and the shrinking layer processor. An activation function that contributes the nonlinear characteristics to the result of the convolution is processed after performing the convolution loops on input feature maps and kernels. Since we completely unroll the convolution loops for input feature maps,

Algorithm 1: Two-stage quantization algorithm

```
Input:  $\mathbf{M}, \mathbf{N}, \mathbf{K}, \mathbf{T}_y$ 
Output:  $\mathbf{best\_M}_q = \{M_q^0, \dots, M_q^{L-1}\}$ ,  $\mathbf{best\_K}_q = \{K_q^0, \dots, K_q^{L-1}\}$ 
1  $\mathbf{G}_M, \mathbf{G}_N, \mathbf{G}_K, \mathbf{G}_{T_y} = \text{Group}(\mathbf{M}, \mathbf{N}, \mathbf{K}, \mathbf{T}_y)$ 
2  $R = \text{receptive\_fields}(K^0, \dots, K^{L-1});$ 
3  $R_0 = R;$ 
4  $\mathbf{G}_K^q[0:2] = \mathbf{G}_K[0:2];$ 
5 for ( $i = 0; R - R_i < \text{threshold}_1; i = i + 1$ ) do // First stage.
6    $n = \text{numDSP}(\mathbf{G}_M[1:2], \mathbf{G}_N[1:2], \mathbf{G}_K[1:2], \mathbf{G}_{T_y}[1:2]);$ 
7    $\mathbf{G}_M^q[1] = \text{feature\_quantization}(\mathbf{G}_M[1], n);$ 
8   for ( $j = 0; j < \text{threshold}_2; j = j + 1$ ) do // Second stage.
9      $\mathbf{G}_q[1] = \mathbf{G}_q[1] - j;$ 
10     $n = \text{numDSP}(\mathbf{G}_M[0:2], \mathbf{G}_N[0:2], \mathbf{G}_K[0:2], \mathbf{G}_{T_y}[0:2]);$ 
11     $\mathbf{G}_M^q[0] = \text{feature\_quantization}(\mathbf{G}_M[0], n);$ 
12     $\text{model} = \text{training}(\mathbf{G}_M^q[0:2], \mathbf{G}_K^q[0]);$ 
13     $\text{best\_model} = \text{compare}(\text{model}, \text{best\_model});$ 
14     $\mathbf{G}_K^q[0:2] = \text{kernel\_quantization}(\mathbf{G}_K[0:2]);$ 
15     $R_{i+1} = \text{receptive\_fields}(\mathbf{G}_K^q);$ 
16 best\_M}_q, \mathbf{best\_K}_q = \text{extract}(\text{best\_model});
```

output feature maps, and kernels, PReLU [15], the modules for activation function of FSRCNN and FSRCNN-s, are designed as many as the number of the output feature maps. Therefore, the output feature maps generated by the CLP of the forward layer can be directly sent to the CLP of the shrinking layer without being stored in the output buffer. Similarly, Figure 4 shows another combined CLP with the merging of the expanding layer processor and the backward layer processor. Large amounts of feature maps generated in the expanding layer must be stored in the same number of line buffers as the width of the kernel size in the backward layer. Instead, we solve this problem by setting T_y^{L-2} in the expanding layer processor to the width of the kernel size in the backward layer. Although the number of line buffers in the expanding layer increases to the width of the kernel size in the backward layer, the efficiency of the on-chip memory can be increased because it stores the smallest feature maps in FSRCNN and FSRCNN-s.

Through this combined CLP architecture, FSRCNN and FSRCNN-s can reduce the required memory size by 3.62 times and 7.67 times compared with the fusion architecture [9].

3.3 MAC Optimization of DCNN accelerator

The state-of-the-art DCNN accelerator reduces the kernel size of the deconvolutional layer from $K_D \times K_D$ to $K_C \times K_C$ and increases the size of the output feature maps from M_D to $M_D \times S_D \times S_D$ through the TDC method, where K_D and K_C denote the width of the kernel size of the deconvolutional layer and transformed convolutional layer, respectively, and M_D and S_D represent the size of output feature maps and the stride of the deconvolutional layer, respectively. As a result, the total number of weights in the transformed convolutional layer is $K_C \times K_C \times S_D \times S_D \times M_D \times N_D$, where N_D denotes the size of the input feature maps in the

deconvolutional layer. However, since the TDC method maps the $K_D \times K_D$ weights to a matrix of $K_C \times K_C \times S_D^2$ size in each input and output feature maps, zero coefficients always occurs in the matrix. The number of zero coefficients, num_{zero} , in the transformed convolution kernels is derived by Equation (3).

$$\text{num}_{zero} = K_C^2 \times (M_D \times S_D^2) \times N_D - K_D^2 \times M_D \times N_D \quad (3)$$

Therefore, when computing the convolution between input blocks and kernels in deconvolutional layer processor, we can reduce the use of FPGA resources by skipping the computations when weights are zero. Specifically, we reduce the DSP usage to 81% in FSRCNN and FSRCNN-s, compared to the TDC method when the kernel size of the deconvolutional layer is 9×9 .

4 MODEL QUANTIZATION

To optimize the utilization of the FPGA resources more compactly, pixels, weights and partial sums are expressed as 16-bit fixed points from the 32-bit single-precision floating points using the bit-width quantization method [16]. The number of DSPs required for the multiplier and adder of the Xilinx Kintex-7 FPGA with the precision of a 16-bit fixed point is one each. If the multiplier and adder are implemented as logic elements in FPGA, the required resources are 280 LUT6s and 16 LUTs+16 FFs, respectively. When completely unrolling several convolution loops, we cannot use both multipliers and adders as DSPs due to the limited number of DSPs. Therefore, we design an adder with LUTs and FFs that require the lower number of logic elements than a multiplier, and a multiplier with a DSP. Therefore, the total number of DSPs required to design the multi-CLPs is as follows.

$$\text{num}_{DSP} = \sum_{l=0}^{L-1} T_y^l \times M^l \times N^l \times K^l \times K^l - \text{num}_{zero} \quad (4)$$

where tiling parameter T_y^l used for the expanding layer is K^{L-l} when l is the order of the expanding layer, $L-2$, and 1 for other cases. In addition, the deconvolutional layer processor performs the optimized MAC through the proposed method, and hence, num_{DSP} is subtracted by the number of zero coefficients.

Therefore, the number of available DSPs is increased. When the layer configurations of FSRCNN and FSRCNN-s are substituted into Equation (4), the number of DSPs required is 16,216 and 5,185, respectively, which are higher than the total number of DSPs in the high-performance FPGAs. Therefore, the two-stage quantization algorithm is proposed to reduce the model size of FSRCNN and FSRCNN-s. Algorithm 1 represents the pseu-do code for the two-stage quantization algorithm. It is used to find the best CNN model that can be implemented in the target FPGA.

In the first stage, we calculate the size of a receptive field to figure how many surrounding pixels are used. The receptive field R has the size of the input block required to generate the pixel for the output feature maps of the last layer. Typically, the performance of the SR is improved as R increases [2, 11, 12], thereby selecting the optimal number considering the performance. R can be calculated in Equation (5).

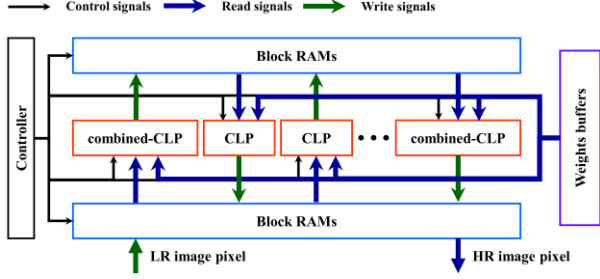


Figure 5: Block diagram of the CNN acceleration system

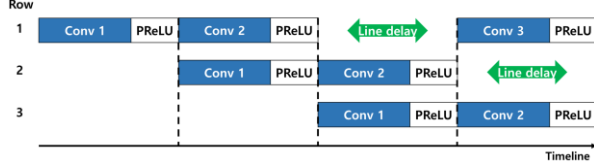


Figure 6: Convolutional layer pipeline

$$R = K^0 + 2 \times \sum_{l=1}^{L-1} \left\lfloor \frac{K^l}{2} \right\rfloor \quad (5)$$

By Equation (5), the size of the receptive field in FSRCNN and FSRCNN-s are 17×17 and 11×11 , respectively. We need to find the best receptive field among the various cases in the first stage. However, as there are many configurations, we limit the size of the receptive field using *threshold*₁.

After that, we define the fundamental problem for designing SR to maximize the performance and implement it in the target FPGA can be formulated as follows.

$$\text{maximize } PSNR_i, \quad \text{s. t. } num_{DSP_i} \leq total \text{ DSPs} \quad (6)$$

where $PSNR_i$ is a peak signal-to-noise (PSNR) value for the i th combination of possible configurations and num_{DSP_i} is the number of DSPs needed at that time. The constraints on the memory are not included because the combined CLP architecture solves them.

Since the object function $PSNR_i$ is calculated by the CNN model obtained through training, an exhaustive search must be performed for all configurations to find the optimal quantized model. In CNN-based SR algorithms, the output feature maps between layers are nonlinearly connected and the performance increases as the number of connections increases [10, 11]. Therefore, we simply change the object function to the function considering the total number of connections in FSRCNN and FSRCNN-s. The problem is reformulated as follows.

$$\text{maximize } \prod_{l=0}^{L-1} M^l, \quad \text{s. t. } num_{DSP} \leq total \text{ DSPs} \quad (7)$$

There is a problem that the variable M^l in the object function is as many as the number of layers in the CNN. We solve the problem by grouping layers with similar characteristics. The total number of connections depends on the size of the output feature maps in each layer. Unlike other layers, the output feature maps of the deconvolutional layer are excluded from the quantization because

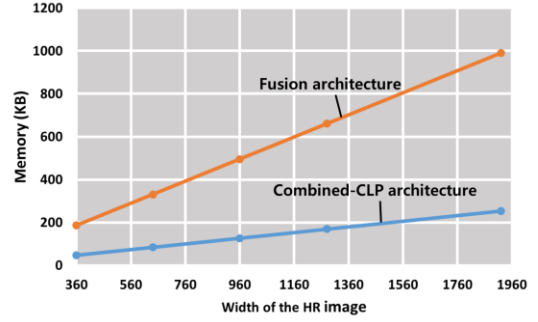


Figure 7: Comparison between the fusion architecture and the combined CLP architecture

each feature maps are merged into HR image. We describe the differential of the connections by the feature maps as dC/dM . Except for the deconvolutional layer, there are an even number of layers with equal dC/dM in the hourglass type FSRCNN and FSRCNN-s. We can represent a set of layers with the same dC/dM and create vectors containing their configurations. For example, in FSRCNN-s, the first layer and the fourth layer have the same dC/dM but are smaller than the other layers. So, the layers belong to the set $\mathbf{G}[0]$ and the layer configurations are stored in $\mathbf{G}_M[0]$, $\mathbf{G}_N[0]$, $\mathbf{G}_K[0]$, and $\mathbf{G}_{Ty}[0]$, respectively, representing vectors of including the tiling parameters, where a set with a higher index value has a larger value of dC/dM than a set with lower index value.

Therefore, we solve the objective function separately for each set. Thus the constraint problem for quantizing the output feature maps of the p th group can be expressed as below:

$$\text{maximize}_{M_q} (M_q)^{N_p}, \quad \text{s. t. } (\alpha \times M_q) + \beta \leq total \text{ DSPs} \quad (8)$$

where M_q is a variable in which the output feature maps are quantized, and N_p is the number of layers having the same size of feature maps. α is the sum of the remaining multiplied configurations and β is the number of DSPs for the layers in the other sets.

Since N_p is an even number, the object function becomes a convex downward. Therefore, the maximum integer satisfying the constraint becomes the solution. The result of the quantized feature maps M_q is as follows.

$$M_q = \left\lfloor \frac{total \text{ DSPs} - \beta}{\alpha} \right\rfloor \quad (9)$$

Consequently, in the second stage, we first quantize the output feature maps $\mathbf{G}_M[1]$ of the layers belonging to the set $\mathbf{G}[1]$ without considering the output feature maps $\mathbf{G}_M[0]$. Then, the output feature maps of the layers belonging to $\mathbf{G}[0]$ are strongly quantized. Since then we increments $\mathbf{G}_M[0]$ by gradually decrementing the values of $\mathbf{G}_M[1]$ until the loop iterator is greater than the *threshold*₂. We repeat this process with the first stage and find the best model. As a result, we reduce the combination of the feature maps in FSRCNN from $\langle 56, 12, 12, 12, 12, 12, 56, S_B^2 \rangle$ to $\langle 23, 3, 3, 3, 3, 3, 23, S_B^2 \rangle$. And we reduce the kernel size of both the first layer and

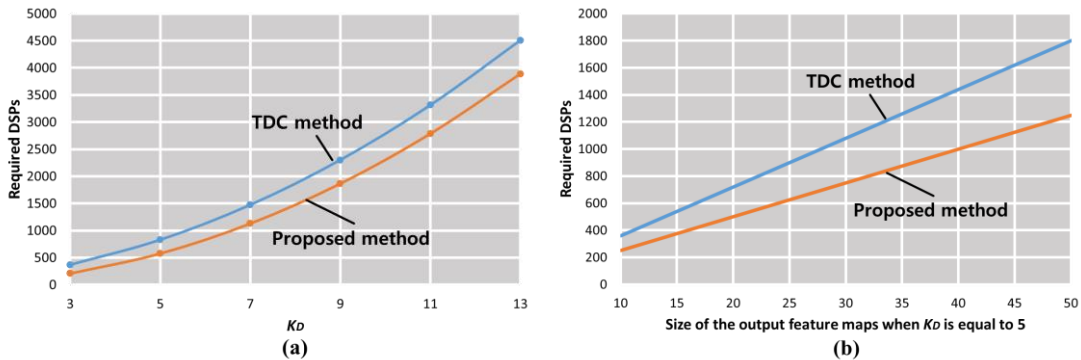


Figure 8: Comparison of DSP utilization between TDC method and proposed method in the FSRCNN

Table 1: Comparison of between the proposed method and the conventional method

| | BRAM | DSP | FF | LUT | Cycles($\times 10^6$) |
|------|------|-------|---------|---------|-------------------------|
| [9] | 574 | 2520 | 151,395 | 142,711 | 33.17 |
| Ours | 120 | 1,491 | 53,242 | 45,279 | 0.92 |

the last layer in FSRCNN from 5×5 to 3×3 . The PSNR is 36.28dB, which is 0.72dB lower than the original model in a Set5 test dataset.

5 EXPERIMENTAL RESULTS

We evaluated the proposed on-chip CNN accelerator using the Xilinx Kintex-7 410T FPGA. We designed it with Verilog RTL through Vivado 2016.4 shown in Figure 5. The CLP of the first layer and the CLP of the second layer, the shrinking layer, were fused to the combined CLP. In addition, the expanding layer and the final layer, which was the deconvolutional layer, were fused to another combined CLP. Therefore, intermediate data that required lots of memory in the each combined CLPs were not stored. In addition, weight buffers were stored in ROM because it operated as read only. Our system had the scale factor of 2 and rendered the QHD images from input image of 1280×720 pixel resolution. Table 1 shows the resources utilization of the proposed accelerator. Our accelerator used a small amount of FPGA resources compared to [9]. We set working frequency of the FPGA as 100MHz. The execution times for generating FHD, QHD, and UHD images were 5.28ms, 9.21ms, and 20.73ms, respectively. Thus its rendering speed was 36 times higher than of the conventional method.

Figure 6 shows that the layers in the CNN are performed on the pipeline through the proposed accelerator. Thus, all layer were performed concurrently on the same timeline. For layers with the width of the kernel size greater than 1, a line delay was generated until the line buffers equal to the size of T_k^l was filled. Exceptionally, the expanding layer generated a line delay for the combined CLP. In the PReLU, the output of the convolution was added to the bias, and when it was smaller than 0, the result was multiplied by the PReLU coefficients. So, we implemented adders and multipliers through logic elements for every PReLU module. Figure 7 shows the amount of memory required to implement the

on-chip CNN accelerator using the fusion architecture and the combined CLP architecture for the quantized FSRCNN. The fusion architecture required about 1MB of the on-chip memory when generating UHD images, while the proposed method required 250KB of memory, which was four times less than that of the fusion architecture. Therefore, we could solve the conventional problem that required lots of memory to store feature maps. Figure 8 shows the comparison of DSP usage between the TDC method and the proposed method in the deconvolutional layer. In Figure 8 (a), if K_D was 5, the difference in DSP usage between the two methods was about 500. We could also found that the larger the feature maps, the higher the difference in Figure 8 (b). This enormous difference was an important factor in designing the CNN accelerator. Because the CNN accelerators should process the convolutional layers and the deconvolutional layer as fast as possible with a limited amount of DSPs in the FPGA. Therefore, the proposed method could operate much more effectively than the conventional method in limited hardware resources.

6 CONCLUSIONS

In this paper, we proposed a novel on-chip CNN accelerator to solve the limitation due to the off-chip data transfer. We implemented the FSRCNN, well known as CNN-based SR, using Xilinx Kintex-7 FPGA. We developed the 2-stage quantization technique to implement the limited FPGA resources. In experimental results, our on-chip CNN accelerator generated HR images in real time. In addition, we reduced the on-chip memory usage and DSP usage by 4 times and 1.44 times, respectively, compared to conventional methods.

REFERENCES

- [1] A. Krizhevsky, I. Sutskever, and G. E. Hinton. 2012. Imagenet classification with deep convolutional neural networks. *In NIPS '12.*
- [2] C. Dong, C. C. Loy, K. He, and X. Tang. 2014. Learning a deep convolutional network for image super-resolution. *In ECCV '14.* 184-199.
- [3] C. Zhang, P. Li, G. Sun, Y. Guan, B. Xiao, and J. Cong. 2015. Optimizing FPGA-based Accelerator Design for Deep Convolutional Neural Networks. *In FPGA '15.* 161-170.
- [4] Y. Ma, Y. Cao, S. Vrudhula, and J.-S. Seo. 2017. Optimizing Loop Operation and Dataflow in FPGA Acceleration of Deep Convolutional Neural Networks. *In FPGA '17.* 45-54.
- [5] Y. Shen, M. Ferdman, and P. Milder. 2017. Maximizing CNN Accelerator Efficiency Through Resource Partitioning. *In ISCA '17.* 535-547.

- [6] M. Alwani, H. Chen, M. Ferdman, and P. Milder. 2016. Fused-layer CNN accelerators. *In MICRO '16*. 1-12.
- [7] H. Yonekawa and H. Nakahara. 2017. On-Chip Memory based Binarized Convolutional Deep Neural Networks Applying Batch Normalization Free Technique on an FPGA. *In IPDPSW '17*. 98-105.
- [8] Q. Xiao, Y. Liang, L. Lu, S. Yan, and Y.-W. Tai. 2017. Exploring Heterogeneous Algorithms for Accelerating Deep Convolutional Neural Networks on FPGAs. *In DAC '17*. 62.
- [9] J.-W. Chang and S.-J. Kang. 2018. Optimizing FPGA-based Convolutional Neural Networks Accelerator for Image Super-Resolution. *In ASP-DAC '17*.
- [10] R. Keys. 1981. Cubic convolution interpolation for digital image processing. *IEEE Transactions on acoustics, speech, and signal processing*, 1981. 1153-1160.
- [11] C. Dong, C. C. Loy, and X. Tang. 2016. Image Super-Resolution using Deep Convolutional Networks. *IEEE Trans. pattern analysis and machine intelligence '16*. 295-307.
- [12] C. Dong, C. C. Loy, and X. Tang. 2016. Accelerating the super-resolution convolutional neural networks. *ECCV '16*. 391-407.
- [13] S. Han, H. Mao, and W. J. Dally. 2015. Deep compression: Compressing deep neural networks with pruning, trained quantization and Huffman coding. *arXiv preprint arXiv:1510.00149*, 2015.
- [14] Xilinx, 7 series FPGAs memory resources user guide.
- [15] K. He, X. Zhang, S. Ren, and J. Sun. 2015. Delving deep into rectifiers: surpassing human-level performance on imagenet classification. *In ICCV '15*. 1026-1034.
- [16] D. Lin, S. Talathi, and S. Annapureddy. 2016. Fixed point quantization of deep convolutional networks. *In ICML '16*. 2849-2858.